

BayesLands: A Bayesian inference approach for parameter uncertainty quantification in Badlands

Rohitash Chandra^{b,a}, Danial Azam^a, R. Dietmar Müller^b, Tristan Salles^a, Sally Cripps^{b,c}

^aEarthByte Group, School of Geosciences, University of Sydney, NSW 2006
Sydney, Australia

^bCentre for Translational Data Science, University of Sydney, NSW 2006
Sydney, Australia

^cSchool of Mathematics and Statistics, University of Sydney, NSW 2006
Sydney, Australia

Abstract

Bayesian inference provides a principled approach towards uncertainty quantification of free parameters in geophysical forward models. This provides advantages over optimization methods that provide single point estimates as solutions, which lack uncertainty quantification. Badlands (basin and landscape dynamics model) is geophysical forward model that simulates topography development at various space and time scales. Badlands consists of a number of geophysical parameters that need to be estimated with appropriate uncertainty quantification, given the observed ground truth such as surface topography, sediment thickness and stratigraphy through time. This is challenging due to the scarcity of data, sensitivity of the parameters and complexity of the Badlands model. In this paper, we take a Bayesian approach to provide inference using Markov chain Monte Carlo sampling (MCMC). Hence, we present *BayesLands*, a Bayesian framework for Badlands that fuses information obtained from complex forward models with observational data and prior knowledge. As a proof-of-concept, we consider a synthetic and real-world topography with two free parameters, namely precipitation and erodibility, that we need to estimate through BayesLands. The results of the experiments shows that BayesLands yields a promising distribution of the parameters. Moreover, the challenge in sampling due to multi-modality is presented through visualizing a likelihood surface that has a range of suboptimal modes.

Keywords: Bayesian Inference, Forward models, Solid Earth Evolution, Stratigraphic Forward Modelling, Markov Chain Monte Carlo,, Badlands

1. Introduction

A new generation of Earth evolution models has recently emerged with the capability to link models for dynamic and isostatic topography through time [1] with landscape evolution models [2], thus providing a model for landscape evolution in response to surface uplift and subsidence over a large range of spatial scales, and track sediments from source to sink [3, 4]. Geophysical forward models depend on uncertain initial and boundary conditions [5], such as global sea level, spatial and temporal variations in precipitation and rock erodibility [6, 7]. These models are calibrated against ground truth data which include the present-day topography and river geometries, total sediment thickness, sediment stratigraphy (constraining the time-dependence of sedimentation) and sedimentation rates, the time-dependent rock exhumation history from thermochronology data, geologically mapped paleocoastlines and geological data that constraints sediment provenance. Basin and landscape dynamics (Badlands) is an example of a landscape evolution model for simulating topography development at various space and time scales [3].

Bayesian inference provides a principled approach to combining information from various sources to estimate and quantify uncertainty of an unknown parameter via the posterior distribution. Markov Chain Monte Carlo sampling methods (MCMC) implement Bayesian inference that sample from a probability distribution [8, 9]. The Bayesian paradigm, together with MCMC techniques, has enabled the development of flexible complex probabilistic models. The application of Bayesian inference via MCMC methods in Earth science has been demonstrated in a number of papers; characterizing geochronological data that describes the age of rocks and fossils [10]; modelling the effect of climate changes in land surface hydrology [11]; calibrating hydrologic models [12]; flood frequency analysis [13]; inferring sea-level and sediment supply from the stratigraphic record [14]; and inferring groundwater contamination sources [15].

In the past few decades Bayesian methods have become more popular in geophysics [16, 17, 18, 19] where the emphasis has shifted from obtaining optimized point estimates, [20] to providing inference regarding the parameters [21]. However, in the context of landscape (Earth) evolution models, MCMC methods have not been used fuse information given by complex forward models with observational data. Although MCMC is an established methodology, forward models of the Earth's evo-

*Principal corresponding author

Email address: rohitash.chandra@sydney.edu.au (Rohitash Chandra)

lution such as Badlands are characterized by parameters that interact in a complicated fashion, which can feature a high dimensional parameter space. Moreover, the posterior distribution of these parameters may have multiple modes and discontinuities. Moreover, estimating them is also computationally expensive as thousands of samples need to be generated for attaining a posterior distribution. Therefore, due to these challenges, Bayesian inference methods have not been used for Earth evolution models in the past [3, 4]. Although optimization methods are the alternatives, they lack uncertainty quantification, and hence this provides the motivation to use Bayesian inference via MCMC methods.

This paper presents Bayeslands which is a framework for inference and uncertainty quantification in the Badlands model used for basin and landscape evolution. We generate two simulated topographic as ground-truth data in order to test the effectiveness of Bayeslands in inference of the free parameters that include rainfall and erodibility. Furthermore, we compare the performance of different instances of Bayeslands given different resolution for summary statistics or measure of quality of predicted topographies. We evaluate the performance of Bayeslands in terms of prediction of the final elevation and sediment deposition over time. Moreover, we and present a visualization of the respective likelihood surfaces and compare it with the distribution of the free parameters. We employ MCMC random-walk sampler in Bayeslands for inference. This is used because Badlands does not have the feature of providing gradients of the selected parameters, hence the random-walk sampler is most suitable.

2. Background and Related Work

2.1. Bayesian inference

Bayesian inference is a principled way of performing data fusion, where diverse sources of information about the system and the model of the system can be combined [22]. This includes expert opinion, ground-truth data, and knowledge from physical processes and geophysical models [23, 24]. Bayes' rule is central to Bayesian inference which states that prior beliefs about parameters are updated with data as more information becomes available

$$p(\theta|D) \propto p(D|\theta).p(\theta)$$

Where $p(\cdot)$ represents a probability density distribution. Bayes rule states that the probability of θ given the data D (the posterior $p(\theta|D)$) is proportional to the likelihood $p(D|\theta)$ and the prior probability of the parameter θ . The prior probability can be informed by measurements, previous research and expert opinion. Likelihoods are probabilistic models of the data-generating process given some parameters θ . They are used to describe how likely the data is given a value of θ . The choice of likelihood function depends upon the data.

The posterior density $p(\theta|D)$, is rarely available in closed form, so sampling based methods, such as MCMC, are used to approximate it. Loosely speaking, MCMC uses the Metropolis-Hastings (MH) algorithm whereby draws of θ are obtained from

some proposal distribution, which are then accepted with a probability which ensures the Markov chain satisfies the detailed balance condition. If the proposed values are not accepted then the chain stays at its current value. Under certain conditions these draws of θ will and converge to draws from the stationary distribution $p(\theta|D)$. Examples of proposal distributions include the Random Walk Metropolis-Hastings (RWMH), the Gibbs Sampler, and the No U-Turn (NUTS) sampler of Hamiltonian MCMC. Open-source Bayesian statistical packages (e.g. pyMC [25]) and those with user interfaces [26]) have made the implementation of MCMC methods easier for researchers without a background in Bayesian statistics.

2.2. Basin and landscape dynamics

Over the last decades, many numerical models have been proposed to simulate how the Earth surface has evolved over geological time scales in response to different driving forces such as tectonics or climatic variability [27, 28, 29, 30, 31]. These models combine empirical data and conceptual methods into a set of mathematical equations that can be used to reconstruct landscape evolution and associated sediment fluxes [32, 33]. They are currently used in many research fields such as hydrology, soil erosion, hillslope stability and general landscape studies.

In this paper, we use *Badlands* [3, 34, 4] to simulate the Earth's surface and our main objective centres around the estimation, with uncertainty quantification, of the parameters in *Badlands*. The *Badlands* framework is intended to simulate regional to continental sediment deposition and associated sedimentary basin architecture [32, 4] (Fig. 1). In its most simple formulation, the Earth surface elevation changes in response to the interaction of three types of processes, (i) tectonic plate movement, (ii) diffusive processes and the associated smoothing effects, and (iii) water flow and the associated erosion. The change in elevation z w.r.t. time is given by

$$\frac{\partial z}{\partial t} = -\nabla \cdot \mathbf{q}_s + u \quad (1)$$

where u in $m \cdot yr^{-1}$ is a source term that represents tectonic uplift. The total downhill sediment flux \mathbf{q}_s is defined by:

$$\mathbf{q}_s = \mathbf{q}_r + \mathbf{q}_d \quad (2)$$

\mathbf{q}_s is the volumetric sediment flux per unit width ($m^2 \cdot yr^{-1}$). \mathbf{q}_r represents transport by fluvial system and \mathbf{q}_d hillslope processes both in $m^2 \cdot yr^{-1}$.

2.2.1. Fluvial system

Badlands uses a triangular irregular network (TIN) to solve the geomorphic equations presented below [35]. The continuity equation is defined using a finite volume approach and relies on the method described in Tucker et al. [36].

To solve channel incision and landscape evolution, the algorithm follows the O(n)-efficient ordering method from Braun and Willett [37] and is based on a single-flow-direction (SFD)

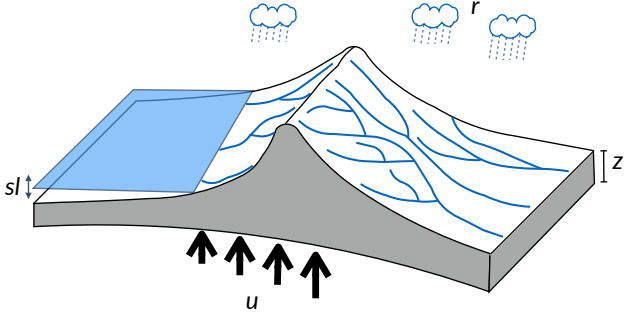


Figure 1: A schematic of two-dimensional landscape evolution model with the main landscape variables and forces: z is the surface elevation, r refers to rainfall, sl to sea-level fluctuations and u to tectonic uplift.

approximation assuming that water goes down the path of the steepest slope [38].

Several formulations of river incision have been proposed to account for long term evolution of fluvial system [28, 39]. These formulations describe different erosional behaviours ranging from detachment-limited incision, governed by bed resistance to erosion, to transport-limited incision, governed by flow capacity to transport sediment available on the bed. Mathematical representation of erosion processes in these formulations is often assumed to follow a stream power law [40]. These relatively simple approaches have two main advantages. First, they have been shown to approximate the first order kinematics of landscape evolution across geologically relevant timescales ($>10^4$ years). Second, neither the details of long term catchment hydrology nor the complexity of sediment mobilisation dynamics are required. However, other formulations are sometimes necessary when addressing specific aspects of landscape evolution.

In this study we use the default fluvial incision law available in *Badlands* which is based on the detachment-limited stream power law, in which erosion rate $\dot{\epsilon}$ depends on drainage area A (m^2), net precipitation P (m/yr) and local slope S and takes the form:

$$\dot{\epsilon} = \kappa_f [PA]^m S^n \quad (3)$$

κ_f is a dimensional coefficient describing the erodibility of the channel bed as a function of rock strength, bed roughness and climate, m and n are dimensionless positive constants. Default formulation assumes $m = 0.5$ and $n = 1$. Using this incision law, sediment deposition occurs solely in topographically closed depression and marine locations.

2.2.2. Hillslope processes

Along hillslopes, we state that the flux of sediment is proportional to the gradient of topography and a linear diffusion law commonly referred to as soil creep (formulated as a diffusion equation) is used [28, 29]:

$$\frac{\partial z}{\partial t} = \kappa_{hl} \nabla^2 z \quad (4)$$

in which κ_{hl} is the diffusion coefficient and can be defined with different values for the marine and land environments. It en-

capsulates, in a simple formulation, a variety of processes operating over short ranges on the superficial veneer of soils and sediments. κ_{hl} varies as a function of substrate, lithology, soil depth, climate and biological activity.

This minimal set of equations, *Badlands* allows for evaluation of sediment transport, landscape dynamics and sedimentary basins evolution under the influence of climate, sea level and tectonics.

3. Materials and Methods

3.1. Creation of Synthetic Data

In order to evaluate the performance of Bayeslands, we consider two possible synthetic landscapes that have distinct features such as development of river systems and mountain ranges. We call these two synthetic topographies *Crater* and *Continental Margin* which were created as follows;

- *Crater*: We analyse the geomorphological evolution over 15,000 years of a synthetic crater-type topography digital elevation model created by *Badlands*. The size of the crater is 123 by 123 points which spans 0.24 x 0.24 kilometers with a resolution factor of 0.02 kilometer/point. Figure 2 shows the initial and the final topography after 15000 years of evolution by *Badlands*. The final topography will be used as the ground-truth topography.
- *Continental Margin*: The *Continental Margin* topography is typically a 1 arc-minute global relief model of Earth's surface that integrates land topography and ocean bathymetry. We analyse the geomorphological evolution over 500,000 years of a real digital elevation model produced by *Badlands*. The original or initial topography was taken from present day as a grid formed by a set of longitude and latitude values (longitude = 173.7 °E - 174.7 °E, latitude = 41.7°S) - 42.3 °S) which spanned 136 x 123 kilometers. This region featured 91 x 81 points which had a resolution factor of 1.5 kilometers/point. Figure 4 shows the initial and the final or ground-truth topography after 500, 000 years of evolution by *Badlands*.

Table 1 shows the parameter values that were used to create the synthetic ground-truth topography with the above information for the respective problems. We assume the final landscapes are observed in the present, by which we mean that the initial conditions for *Crater* began 15,000 years ago while the corresponding point in time for *Continental Margin* was 500,000 years ago.

We take these synthetic landscapes as two examples of ground-truth against which we calibrate the model performance. The ground-truth or observed topography data (Y^{obs}) refers to the topography of present age, where $t = T_{max}$. The goal of *Bayeslands* is to sample and obtain a posterior distribution of the free parameters that govern *Badlands* to predict a topography that recovers the ground truth topography after T_{max} years of landscape evolution. The performance of our method in correctly

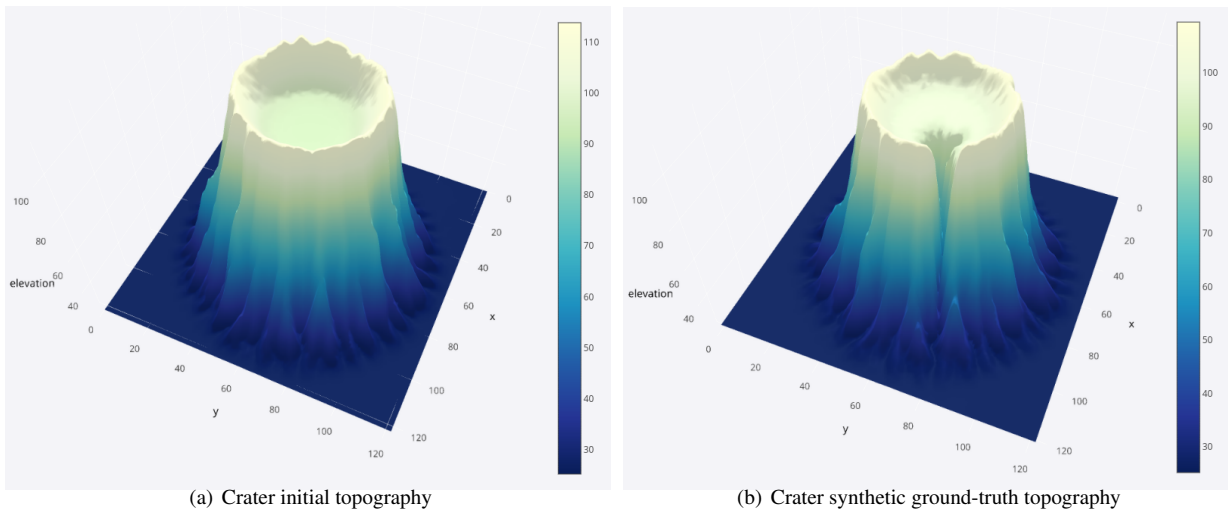


Figure 2: Crater: Initial and eroded ground-truth topography and sediment after 15,000 years.

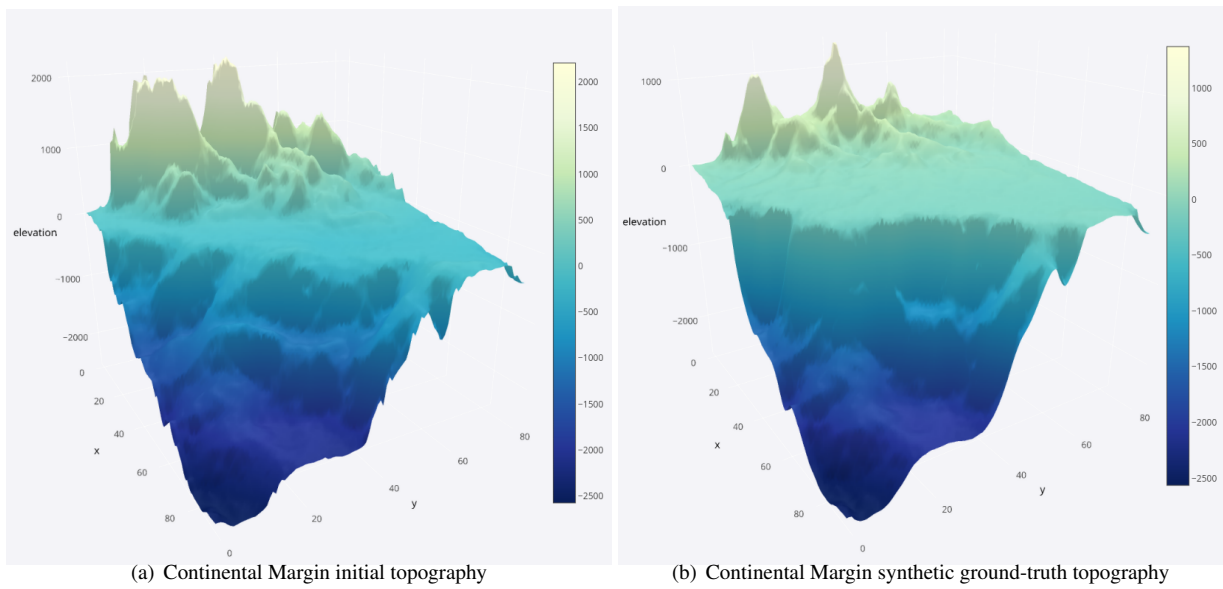


Figure 3: Continental Margin: Initial and eroded ground-truth topography and sediment after 500,000 years.

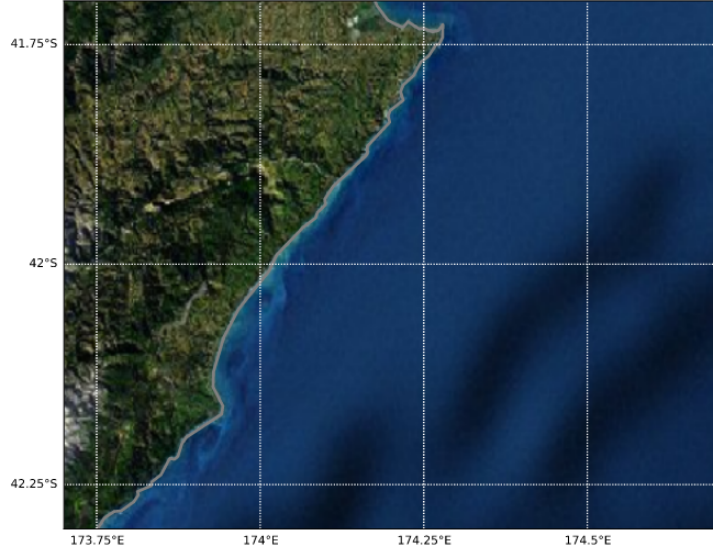


Figure 4: Continental Margin: ARCGIS image of the NE region of the South Island of New Zealand to Basemap.

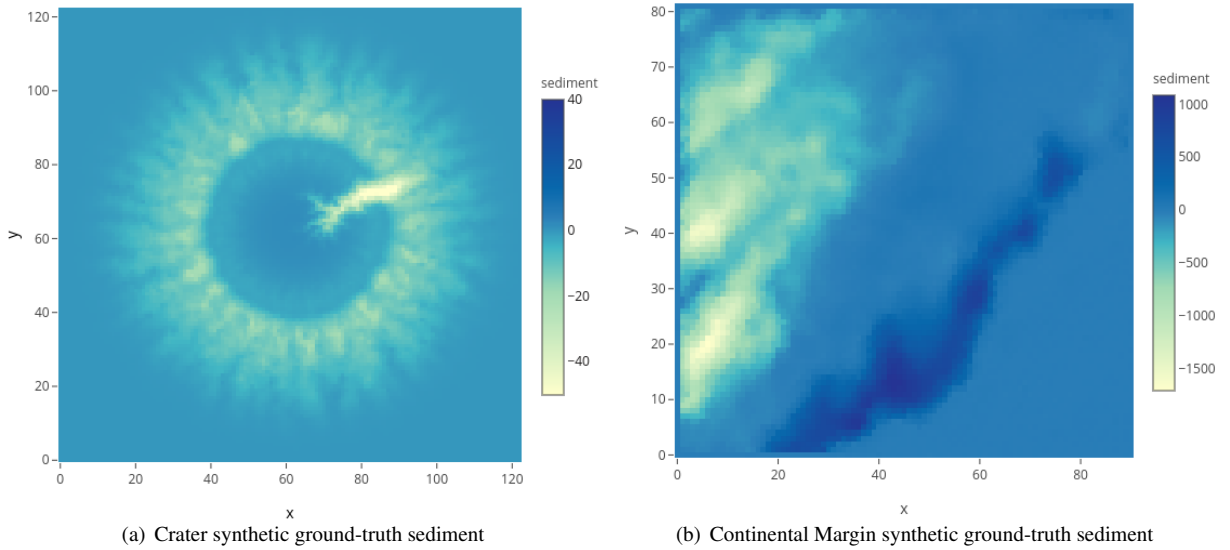


Figure 5: Sediment for Crater and Continental Margin model

Topography	Simulated Time (yrs)	r (m/a)	e	m	n	sd (m ² /a)	md (m ² /a)	rtsd (m ² /a)
Crater	15,000	1.5	5.e-5	0.5	1.0	2.e-2	5.e-2	0.0
Continental Margin	500,000	1.5	5.e-6	0.5	1.0	8.e-1	5.e-1	10.0

Table 1: Experiment configuration. sd: surface diffusion coefficient, md: marine diffusion coefficient, rtsd: river transported sediment diffusion coefficient

predicting the elevation and sediment deposition of the two topographies and also to recover the posterior distributions of the parameters, rainfall and erodibility, used to predict the (simulated) topographies at four intermediate time scales.

3.2. Bayeslands Model and Priors

The Bayeslands framework provides a methodology for estimation and inference of the parameters in the Badlands basin and landscape evolution model. Examples of these parameters are rainfall (m/yr in metres per year) and the erodibility of the landforms. The Bayeslands framework is given in Figure 6.

In order to implement the model, we use take a probabilistic approach and assume that $y_{t,i,j}$, the observed elevation at time t , longitude i and latitude j , is generated from a signal plus noise model,

$$y_{t,i,j} = g_{t,i,j}(\theta) + \epsilon_{t,i,j} \quad (5)$$

where $g(\theta)$, the signal, is the output of the Badlands model given some parameters, θ , and $\epsilon_{i,j} \sim \mathcal{N}(0, \tau^2)$, is the noise, and the notation $N(\mu, \sigma^2)$ refers to the normal distribution with mean μ and variance σ^2 . The noise in (5) reflects the fact that elevation, at any point in time, will be affected by factors (parameters/inputs) other than those in the Badlands model.

Let $\mathbf{Y}_t = (\mathbf{y}_{t,1}, \dots, \mathbf{y}_{t,n})$, where $\mathbf{y}_{t,j} = (y_{t,1,j}, \dots, y_{t,n,j})'$, be the matrix of observed elevations across an $n \times n$ grid of latitude and longitude at time t . The likelihood function of such a model is then

$$P(\mathbf{Y}_t | \theta, \tau^2) = \frac{1}{(2\pi\tau^2)^{n^2}} \exp \left\{ -\frac{\sum_{i=1}^n \sum_{j=1}^n (y_{t,i,j} - g_{t,i,j}(\theta))^2}{\tau^2} \right\} \quad (6)$$

We note that the mean function $g(\theta)$ has no closed form representation in θ . That is, we cannot write down the likelihood as an explicit function of θ , but we note that, given there exists a deterministic relationship between θ and $g(\theta)$, then $P(\mathbf{Y}_t | \theta, \tau^2) = P(\mathbf{Y}_t | g(\theta), \tau^2)$.

To complete the model specification, we need to specify priors for the elements of θ and τ^2 . We take a Jefferies prior [41] for τ^2 and assume $\log(\tau^2) \sim U[0, c_{\tau^2}]$.

$$P(\mathbf{Z}_t, \mathbf{Y}_{T_{max}} | \theta, \tau^2, \sigma^2) = \frac{1}{(2\pi\tau^2)^{n^2}} \exp \left\{ -\frac{\sum_{i=1}^n \sum_{j=1}^n (y_{T_{max},i,j} - g_{t,i,j}(\theta))^2}{\tau^2} \right\} \\ \times \frac{1}{(2\pi\sigma^2)^{n_t m}} \exp \left\{ -\frac{\sum_{t=1}^{n_t} \sum_{j=1}^m (z_{t,j} - f_{t,j}(\theta))^2}{\sigma^2} \right\}$$

where n_t is the number of different times that the sediment thickness is recorded and m is the number of grid points at which the sediment is measured. Table 3 gives the indices that are used to evaluate the likelihood for the erosion deposition (sediment) in 4 successive time intervals.

3.3. Estimation

We take a Bayesian approach and estimate the topography at a particular latitude, longitude and time, T_{max} , by its posterior mean, $E(y_{T_{max},i,j}^* | \mathbf{Z}_t, \mathbf{Y}_{T_{max}})$. The posterior mean is equal to

$$E(y_{T_{max},i,j}^* | \mathbf{Z}_t, \mathbf{Y}_{T_{max}}) = \int E(y_{T_{max},i,j}^* | \mathbf{Y}_{T_{max}}, \theta) p(\theta | \mathbf{Z}_t, \mathbf{Y}_{T_{max}}) d\theta$$

and an estimate of it is

$$\hat{E}(y_{T_{max},i,j}^* | \mathbf{Z}_t, \mathbf{Y}_{T_{max}}) = \frac{1}{M} \sum_{j=1}^M E(y_{T_{max},i,j}^* | \mathbf{Z}_t, \mathbf{Y}_{T_{max}}, \theta^{[j]})$$

where $\theta^{[j]} \sim p(\theta | \mathbf{Y}_{max})$, obtained via MCMC as shown in Algorithm 1 and Figure 6. Inference regarding rainfall and erodibility are via the joint posterior $p(\theta | \mathbf{Y}_{max})$.

In this example, we assume θ consists of the parameters rainfall, θ_1 , and erodibility, θ_2 , which assumed to be constant over time. We place uniform priors on rainfall and erodibility, so that

$$\theta_1 \sim [a_1, b_1]$$

$$\theta_2 \sim [a_2, b_2]$$

where a and b are chosen to represent prior knowledge of rainfall and erodibility for a particular landscape. As stated previously, we only observe landscape elevations in the present day, which we denote by T_{max} . The likelihood given by (6) relates the parameters θ to observed elevations $y_{T_{max},i,j}$. Estimates for surface elevation at previous points in time is not often available; however, sedimentary basins contain a record of the products of erosion, which may be available as total sediment thickness of as a stratigraphic sequence, ie sediment thickness through space and time, for $t < T_{max}$. Therefore, the information from sedimentary deposits can be incorporated into the likelihood. Let $z_{t,i,j}$ be the thickness of the sediment at time t , latitude i , and longitude j . We assume this deposition also depends upon θ via a signal plus noise model whereby

$$z_{t,i,j} = f_{t,i,j}(\theta) + \nu_{t,i,j}$$

where $f(\theta)$, the signal, is the sediment thickness given by the Badlands model, for a given value of θ and $\nu \sim \mathcal{N}(0, \sigma^2)$ is the noise. The likelihood function in (6) can now be expanded to include this information. It becomes

We note that, with only two parameters, it is not too computationally intensive to compute the joint posterior distribution of rainfall and erodibility across a grid (Figure 7). If inference around rainfall and erodibility were all that was required, then we do not need to obtain draws from these distributions. However if we wish to predict and make inference around the topography then we need to be able to draw from these distribution as (7) shows.

There are several options for obtaining these draws, including importance sampling, and many MCMC methods. We have chosen the simple random walk MCMC (RWMCMC) as the vehicle for obtaining these draws because the posterior surface may have many points where the gradient doesn't exist, or is extremely large, and therefore gradient based methods such as the No U-Turn Sampler (NUTS) are not suitable. Our RWMCMC appears in algorithm 1.

Algorithm 1 begins by initializing values of rainfall and erodibility by drawing from their respective prior distributions given in Table 2. Then algorithm then proceeds by proposing new values of rainfall and erodibility from a normal distribu-

tion, centered at the current values and with a covariance matrix chosen by the user. Conditional on these proposed values, Badlands is executed for the maximum time (eg. Crater=15,000 years or Continental Margin=500,000 years) and returns the successive sediments and topographies. The likelihood, given by (7), is calculated by considering the final topography and the successive erosion deposition values at selected coordinates. Once the likelihood is computed, the Metropolis-Hasting criterion is used for determining whether to accept or reject the proposal. If the proposal is accepted, it the chain moves to this proposed value. If rejected, the chain stays at the current value. The process is repeated until the convergence criterion is met, which in this case is the maximum number of samples defined by the user.

Alg. 1 Bayeslands algorithm

Initialize $\theta = \theta^{(0)}$ by drawing $\theta^{(0)}$ from the prior $\theta^{(0)} \sim p(\theta)$

For $i = 1 : Num - Samples$

- 1: Propose a value $\theta^{(p)} | \theta^{(i-1)} \sim q(\theta^{(i-1)})$, where $q(\cdot)$ is the proposal distribution which we choose to be normal with mean $\theta^{(i-1)}$ and covariance matrix, Σ , where Σ is diagonal with entries equal to the square of the step-size.
- 2: Using the forward model *Badlands*, with $\theta^{(p)}$ as the initial conditions, compute $g_{Tmax,i,j}(\theta^{(p)})$, and $f_{i,j}(\theta^{(p)})$
- 3: Calculate:

$$p_{accept} = \min \left\{ 1, \frac{p(\mathbf{Y}_{Tmax}, \mathbf{Z}_i | \theta^{(p)}) p(\theta^{(p)})}{p(\mathbf{Y}_{Tmax}, \mathbf{Z}_i | \theta^{(i-1)}) p(\theta^{(i-1)})} \cdot \frac{q(\theta^{(i-1)} | \theta^{(p)})}{q(\theta^{(p)} | \theta^{(i-1)})} \right\}$$

where $p(\mathbf{Y}_{Tmax}, \mathbf{Z}_i | \theta)$ is given by Equation 7. Note that as $q(\cdot)$ is symmetric and $p(\theta)$ is the product of independent uniform priors, p_{accept} reduces to the likelihood ratio.

- 4: Generate $u \sim U(0, 1)$ and set $\theta^{(i)} = \theta^{(p)}$ if $p_{accept} < u$. Otherwise, set $\theta^{(i)} = \theta^{(i-1)}$.
-

4. Experimental Design and Results

In this section outline the experimental design and report the results. The results are split into three sections. Results of

1. The MCMC sampling scheme.
2. Prediction and inference regarding the landscape and sediment deposits.

Note that the software package in Python along with data files and problems is published online ¹.

4.1. Experimental Design

The Bayeslands framework, given in Figure 6, employs an MCMC random-walk sampler to obtain draws from the joint posterior distribution, in order to predict and make inference regarding the topography.

Table 2 provides information about the experimental setting including information about the MH proposal density's covariance matrix, which is assumed to be diagonal with entries equal to the square of step size. We performed several trial experiments to evaluate an optimum step size for the random-walk sampler.

Note that Badlands takes approximately 1.1 seconds to run a simulation for the Crater, and 0.8 seconds for *Continental Margin* topography. The overall computation time taken for each experimental setup can be found in Table 4. The results were obtained using an Intel Core i7-8700 Processor (Hexa-Core, 8MB, 8T, 3.2GHz). Note that multi-processing was not used in the implementation of MCMC for Bayeslands.

4.2. Results: MCMC

We evaluate Bayeslands for 10,000 and 100,000 samples with a 5% burn-in period. Note that burn-in is considered as the initial sampling period before the draws in the chain are assumed to be from the invariant distribution, which in this case is the joint posterior. The different number of samples are used to check the convergence properties of the MCMC.

Table 4 shows the performance of the respective experimental setup. We judge the accuracy of the prediction by the root mean square error (RMSE), and divide this error between those errors which are attributable to the topography and those that are attributable to the sediment deposits. These quantities are given by

$$RMSE_{elev} = \sqrt{\frac{1}{n^2} \sum_{i=1}^n \sum_{j=1}^n (\hat{g}_{Tmax,i,j} - g_{Tmax,i,j})^2}$$

$$RMSE_{sed} = \sqrt{\frac{1}{n_t m} \sum_{t=1}^{n_t} \sum_{j=1}^m (\hat{f}_{t,j} - f_{t,j})^2}$$

where \hat{g} and \hat{f} are the predicted topography and sediment thickness and g and f are the ground truth topography and thickness, respectively.

Figure 8, panels (a) and (b) show the trace plots of the iterates of rainfall and erodibility in the MCMC scheme for the Crater landscape while Figure 9 has analogous plots for the Continental Margin landscape.

4.3. Results: Prediction and Inference for Topographies and Sediment Deposits

Figure 10 shows the successive predictions for this the crater topography. Figure 12 shows a cross section with uncertainty quantification. Figures 11 and 13 are analogous plots for the Continental Margin landscape.

Figure 15 and Figure ?? show the evolution of sediment thickness, at the selected points, over time for the Crater and Continental Margin landscapes, respectively.

5. Discussion

5.1. MCMC results

Figure 7 contains the true likelihood surface as a function of rainfall and erodibility for both landscapes and shows just

¹Bayeslands: <https://github.com/badlands-model/BayesLands>

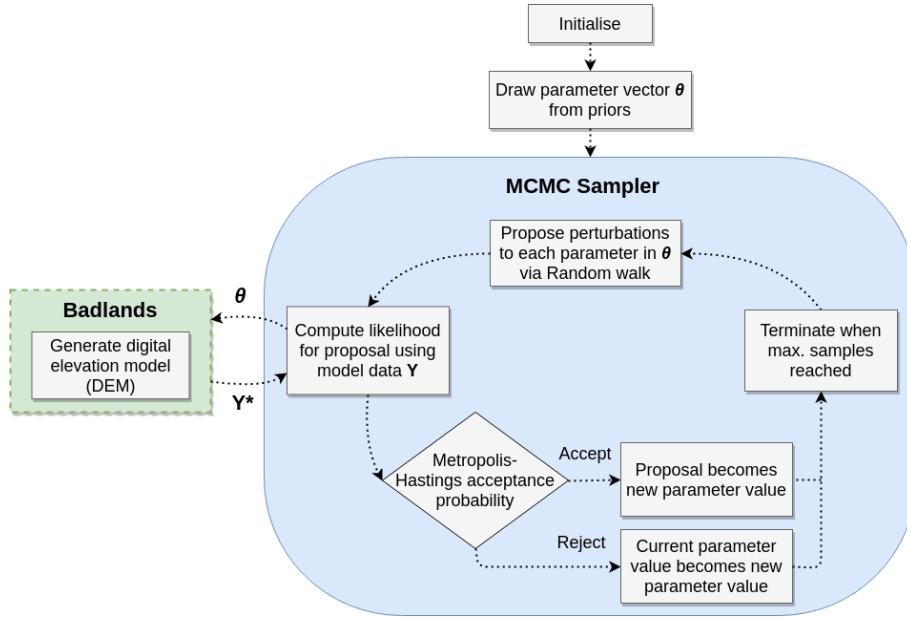


Figure 6: Bayeslands framework employing MCMC random-walk sampler and Badlands model.

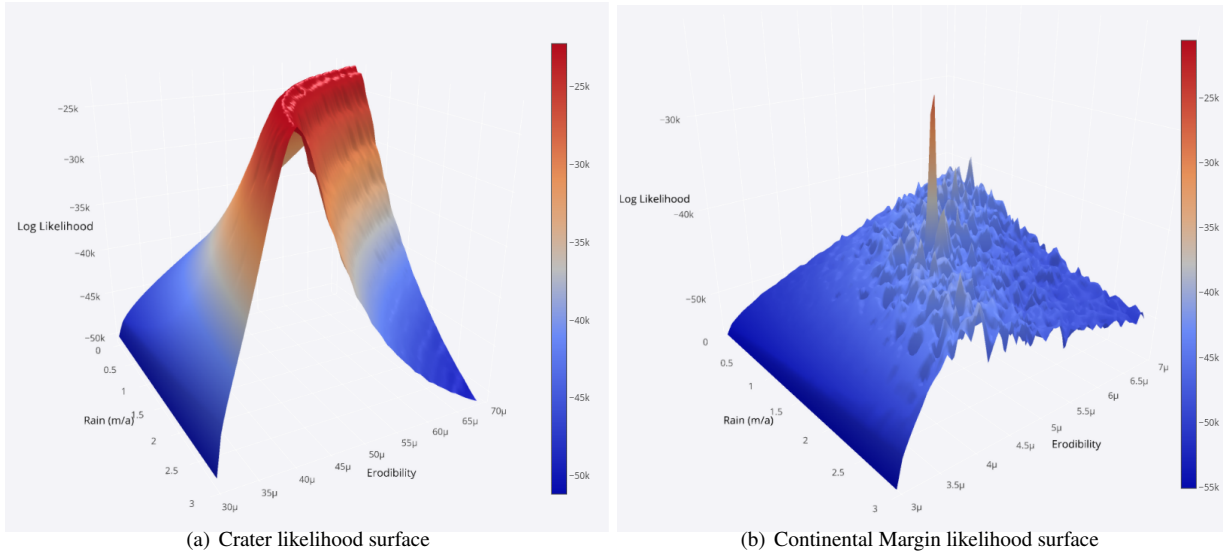


Figure 7: Likelihood Surfaces for Crater and Continental Margin

Topography	Prior range θ_1	Prior range θ_2	step size θ_1	step size θ_2
Crater	[0.0-3.0]	[3.e-5, 7.e-5]	0.03	4.e-7
Continental Margin	[0.0-3.0]	[3.e-6, 7.e-6]	0.03	4.e-8

Table 2: Prior information of free parameters.

Topography	Sediment coordinates
Crater	(42,49), (44,86), (60,60), (72,66), (79,91), (85,73), (88,69), (90,75), (96,77), (100,80)
Continental Margin	(4,40),(6,20),(14,66),(39,8),(40,5),(42,10),(59,13),(68,40),(72,44),(75,51)

Table 3: Erosion deposition (sediment) coordinates used in likelihood evaluation

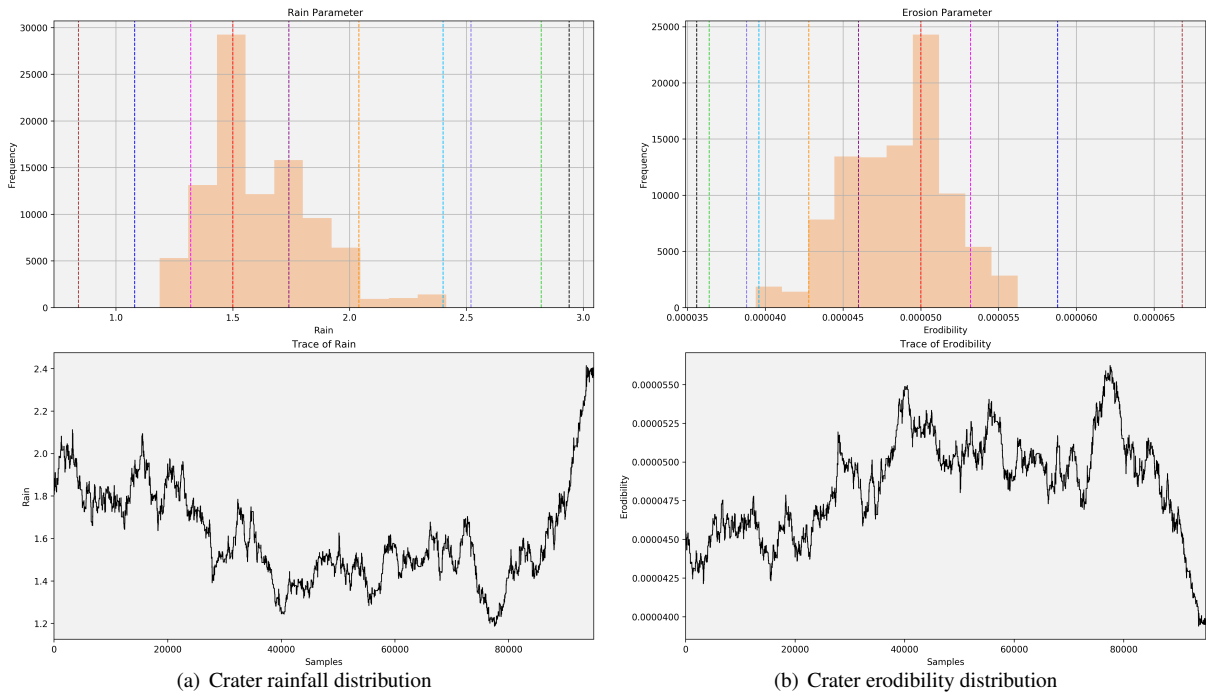


Figure 8: Crater: Posterior distribution and trace plots for rainfall and erodibility

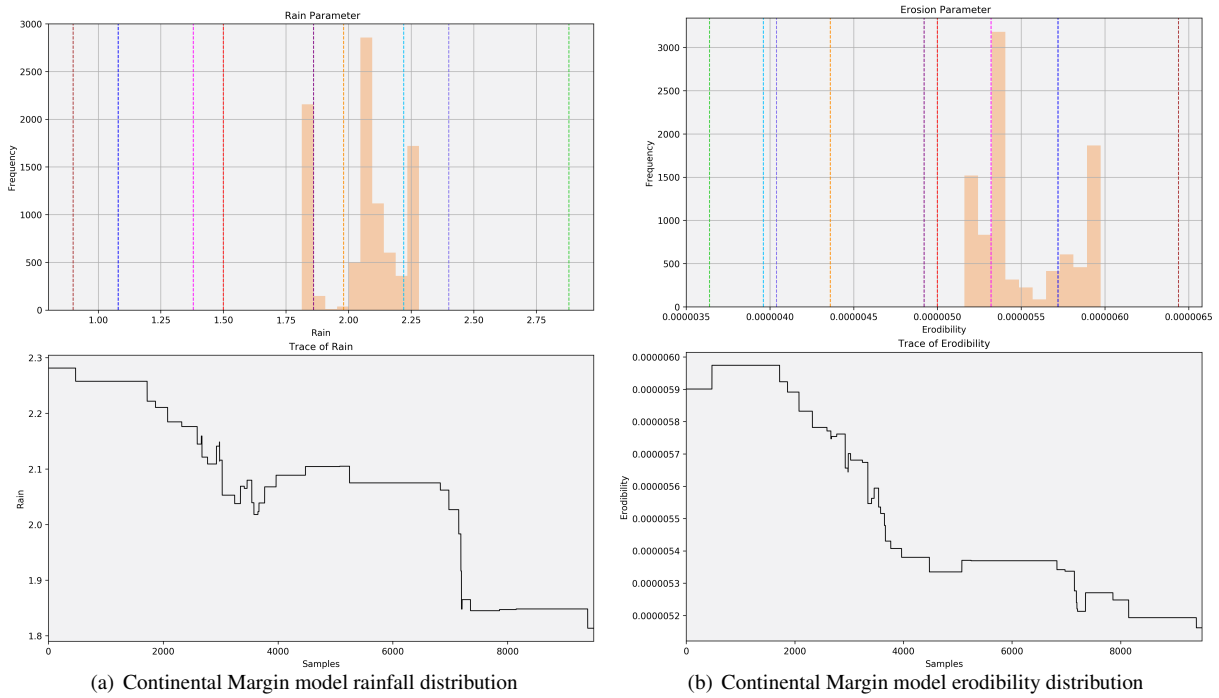


Figure 9: Continental Margin: Posterior distribution and trace plots for rainfall and erodibility

Topography	Samples	Accepted %	Time(hrs)	Pred. RMSE	Elev. RMSE	Sed. RMSE
Crater	10,000	2.350	2.260	9.299	1.055	8.244
Crater	100,000	2.566	17.050	9.298	1.055	8.243
Continental Margin	10,000	0.470	1.680	527.217	67.365	459.851
Continental Margin	100,000	0.023	12.150	398.526	10.604	387.922

Table 4: Results for MCMC random walk sampler

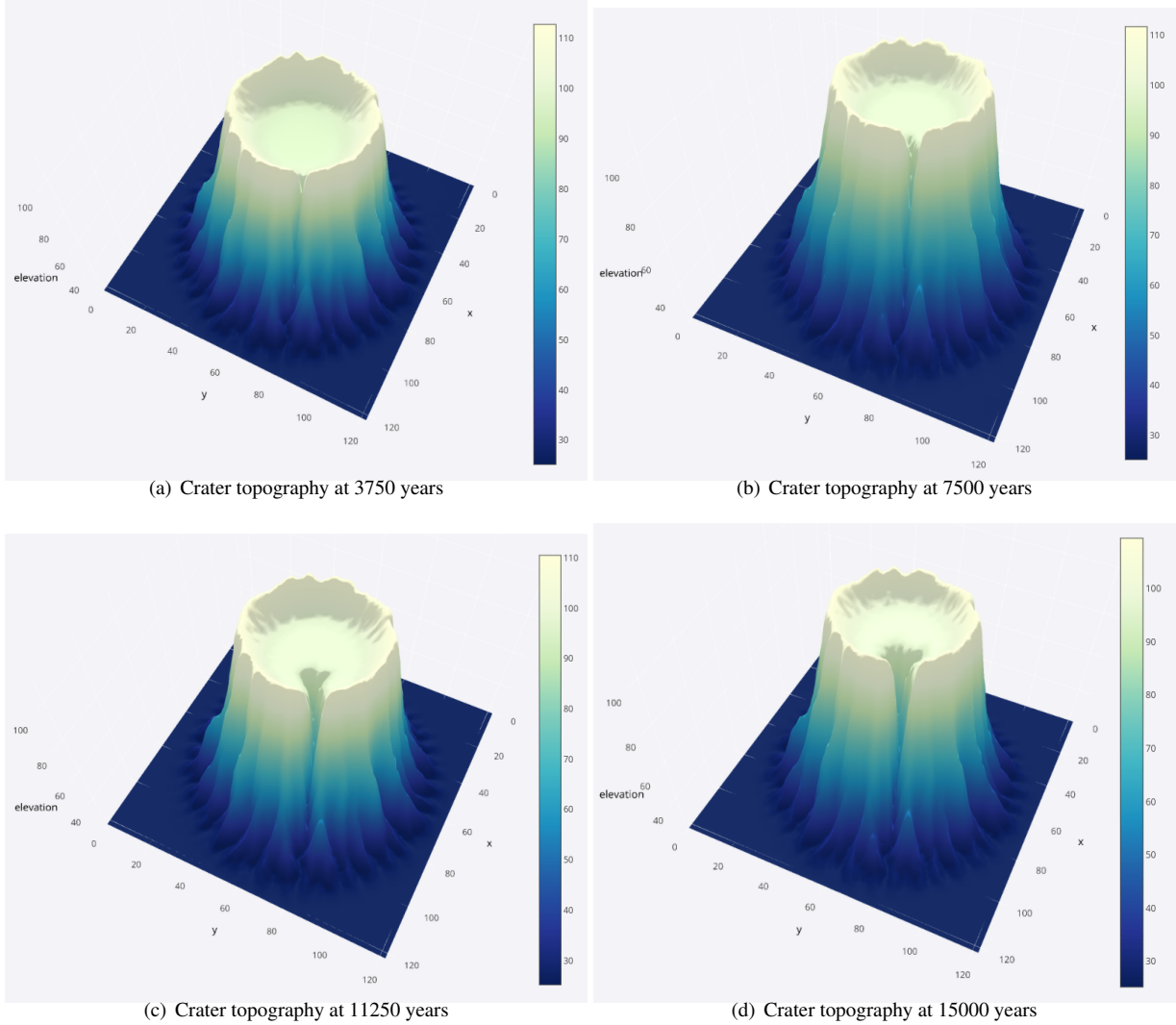


Figure 10: Crater: Predicted topographies at intervals of 3750 years.

how difficult it is to explore these surfaces. Figure 7 panel (a) is the likelihood surface for the Crater landscape and shows that this surface is more sensitive to erodibility than rainfall. It also shows that there is no unique mode for rainfall, with several combinations of rainfall and erodibility giving the same likelihood value, indicated by a ridge.

Figure 7 (b) is the likelihood surface for the landscape, which is a sharp contrast to the likelihood surface for the Crater. Unlike Figure 7 panel (a), Figure 7 (b) shows the existence of a unique global mode but also the existence of many smaller

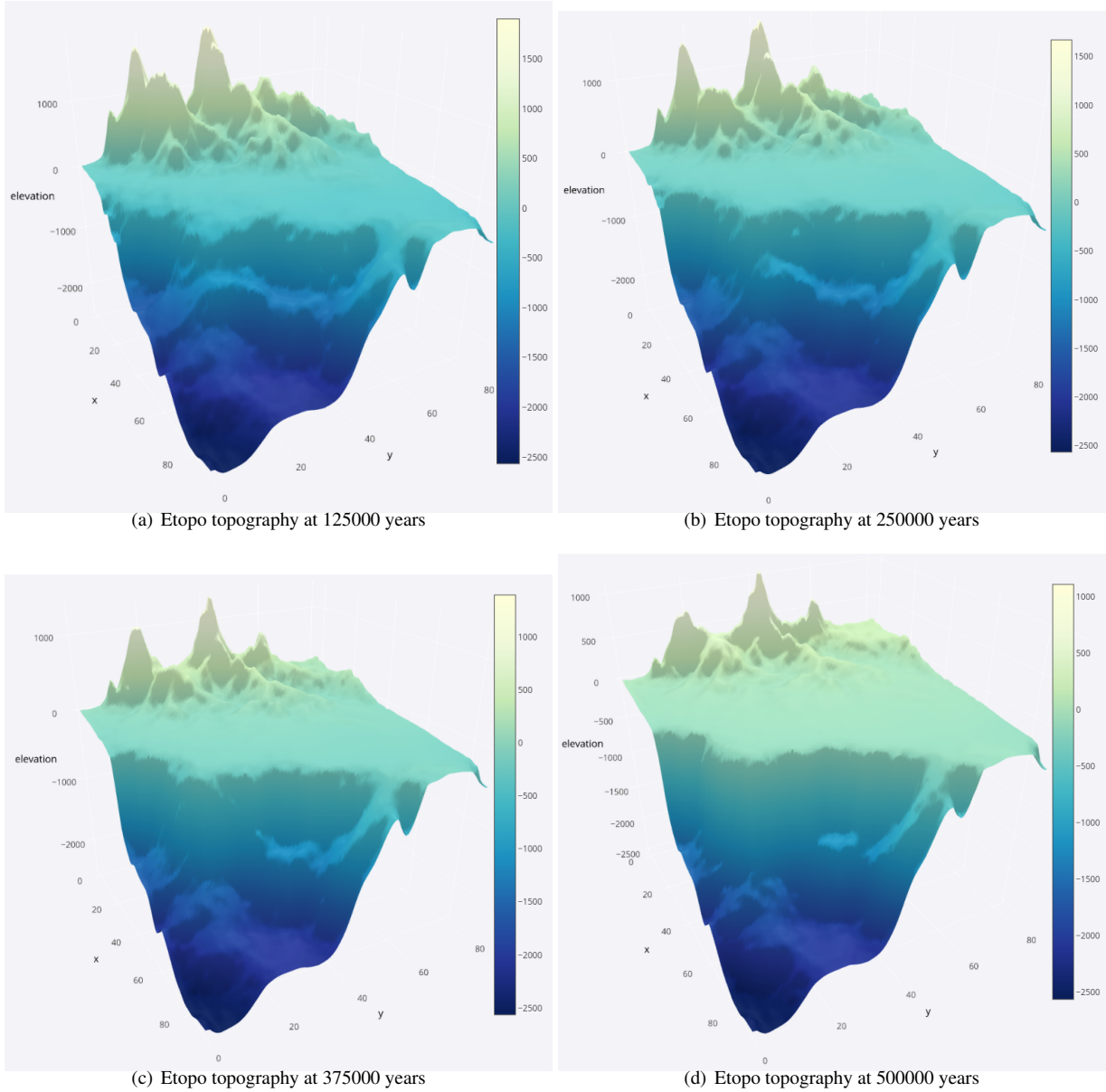


Figure 11: Continental Margin: Predicted topographies at intervals of 125000 years.

modes. These local modes make exploration of the surface very problematic.

Comparing these true posteriors with the estimates produced from the MCMC scheme, Figures 8 and 9, we can see that, for the Crater landscape, the MCMC estimate of the posterior distribution is reasonable. It is peaked at the "true" values of rainfall and erodibility, which is given by the red dashed vertical line and the chain appears to mix well, albeit with a high degree of autocorrelation.

However the same is not true for the Continental Margin landscape. The trace plots in the bottom row of Figure 9, show very little mixing, probably due to the fact that the chain becomes stuck in local modes. The histogram estimates of rainfall and erodibility are not peaked around the "true" values for these

parameters. Instead they are multimodal with modal values corresponding to local maxima, given by the coloured dashed vertical lines. These results are not surprising considering the extremely challenging nature of the surface to be explored.

Table 4 contains summaries statistics for the MCMC schemes, and shows that $RMSE_{total}$ decreased (improved) with the increase in sample size from 10,000 to 100,000 for the Continental Margin topography. This improvement is in both $RMSE_{elev}$ and $RMSE_{sed}$, suggesting that the MCMC scheme for this landscape had not converged within the first 10,000 samples. In contrast $RMSE_{total}$ for the Crater landscape did not significantly change. The difference in these results are not surprising, when one considers that the Continental Margin topography's likelihood function is very complex when compared with that

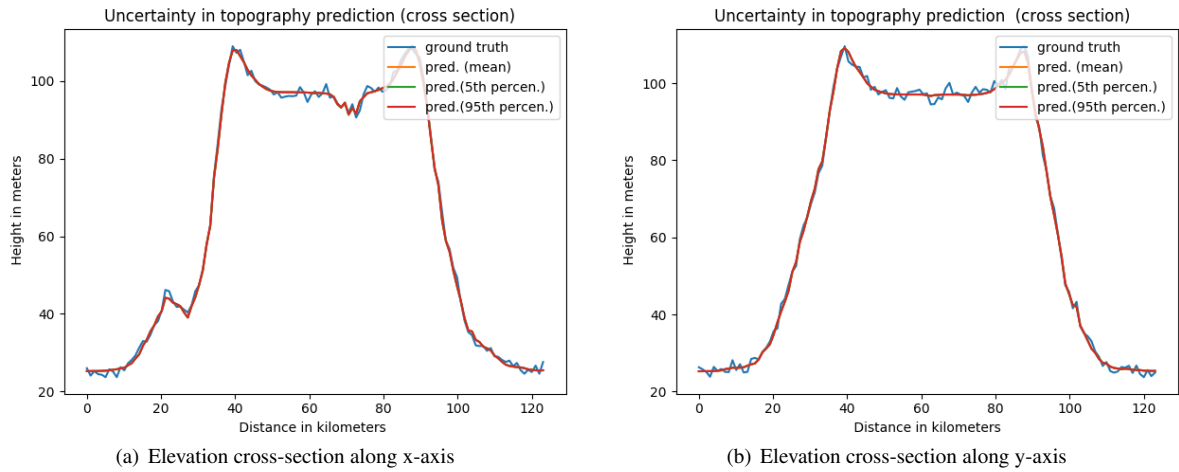


Figure 12: Crater: Elevation cross-section taken at mid-point along x-axis and y-axis

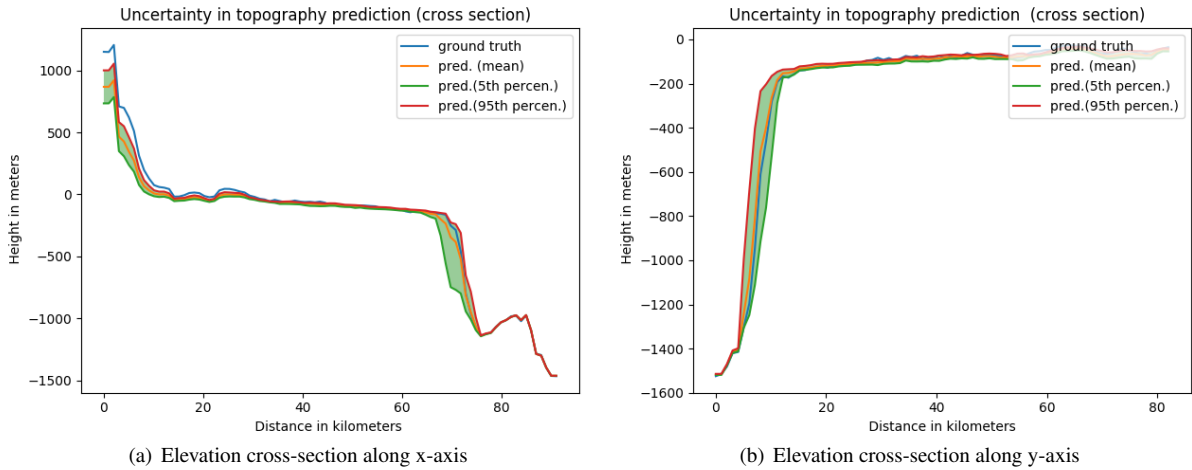


Figure 13: Continental Margin model: Elevation cross-section taken at mid-point along x-axis and y-axis

of the Crater, resulting in the need for longer sampling time to transverse this surface.

5.2. Prediction and inference regarding landscape and sediments

Despite the difficulty in recovering the "true" parameter values, the predictions of the landscapes are astonishingly accurate. This is evident not only from the predicted topography, Figures 10 and 11 which are visually similar to the ground truth, Figures 2 and 4, but also by the cross-sections shown in Figures 12 and 13. Figures 12 and 13 show the 95% credible intervals which highlight the accuracy of the prediction.

Figures 15 and ?? show the predicted evolution of the sediment thickness for both landscapes. Interestingly the predictions for the Continental Margin landscape appear to be more accurate than those of the Crater landscape. However this may be due to the different scales, with the sediment thickness of

the Crater landscape two orders of magnitude less than the sediment thickness of the Continental Margin landscape, and therefore shown on a finer scale, making differences appear larger.

5.3. Limitations and implications

The limitations of the experimental design for Bayeslands is that a uniform rainfall value for the entire spatial or temporal extent of a given model may not be appropriate. While this does not make much difference for small geographical regions and short time intervals, for larger areas, different regions of the topography would have different distributions of rainfall at different points of time. Moreover, the erodibility value is also same throughout the entire topography. This does not fully simulate geological time scales and fully capture the effects of changing climate through time. In order to implement this, the rainfall would become a vector of parameters that define different regions expressed by grids in the map. This would increase the number of parameters and further add complexity to the model

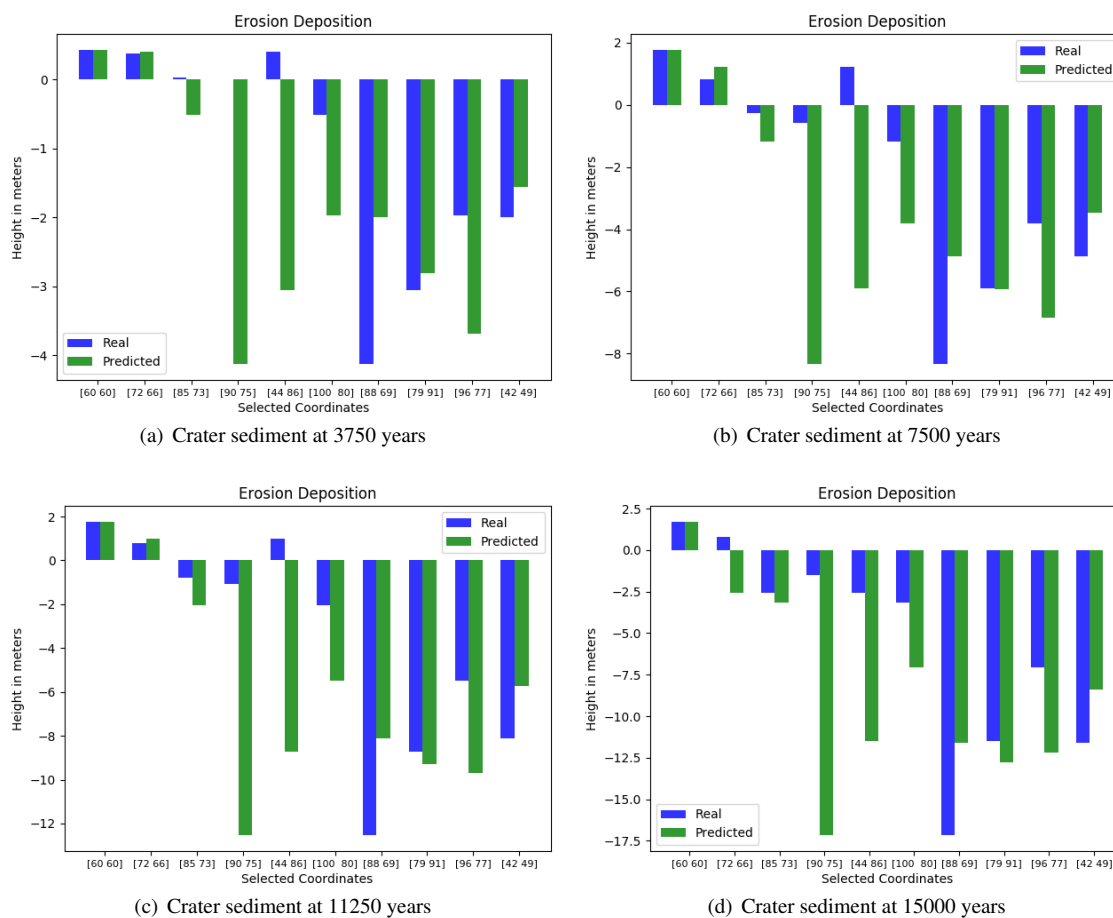


Figure 14: Crater: Sediment erosion and deposition through 15000 years.

which would make the inference more difficult. Furthermore, the synthetic problems should consider larger areas that contain a variety of landscape features. This would increase the computational complexity of the model and require multi-core implementations of MCMC via high performance computing. This naturally appeals to use of parallel tempering [42] which is an advanced MCMC method suited for multi-core implementations with features that better captures multimodality [19, 43].

6. Conclusions and Future Work

The Bayeslands software provides a framework for incorporating uncertainty quantification through sampling in landscape evolution models. The results show that the approach is suitable for attaining a posterior distribution of free parameters that not only gives accurate predictions, but also provides uncertainty quantification for predicted or simulated elevation and sediments using Badlands. Although promising, there are major challenges of the method for future real-world applications. This includes the presence of multi-modal and discontinuous posterior surfaces, which will increase in complexity with higher dimensions. To explore these challenging surfaces will require the development of new proposal distributions for use in

MCMC schemes, which reflect local geometry and/or gradient information from the Badlands model.

These methods are also computationally challenging; Badlands takes minutes to hours for a single proposal for large scale or continental problems. Hence, new computationally efficient methods, such as replacing the Badlands model with surrogate models, in a large proportion of the MCMC iterates needs to be developed. Speeding up computation of Bayeslands via parallel tempering in multi-core architecture is another avenue to be explored in the future.

7. References

References

- [1] N. Flament, M. Gurnis, R. D. Müller, A review of observations and models of dynamic topography, *Lithosphere* 5 (2) (2013) 189–210.
- [2] T. Coulthard, Landscape evolution models: a software review, *Hydrological processes* 15 (1) (2001) 165–173.
- [3] T. Salles, L. Hardiman, Badlands: An open-source, flexible and parallel framework to study landscape dynamics, *Computers & Geosciences* 91 (2016) 77–89.
- [4] T. Salles, N. Flament, D. Müller, Influence of mantle flow on the drainage of eastern australia since the jurassic period, *Geochemistry, Geophysics, Geosystems* 18 (1) (2017) 280–305.

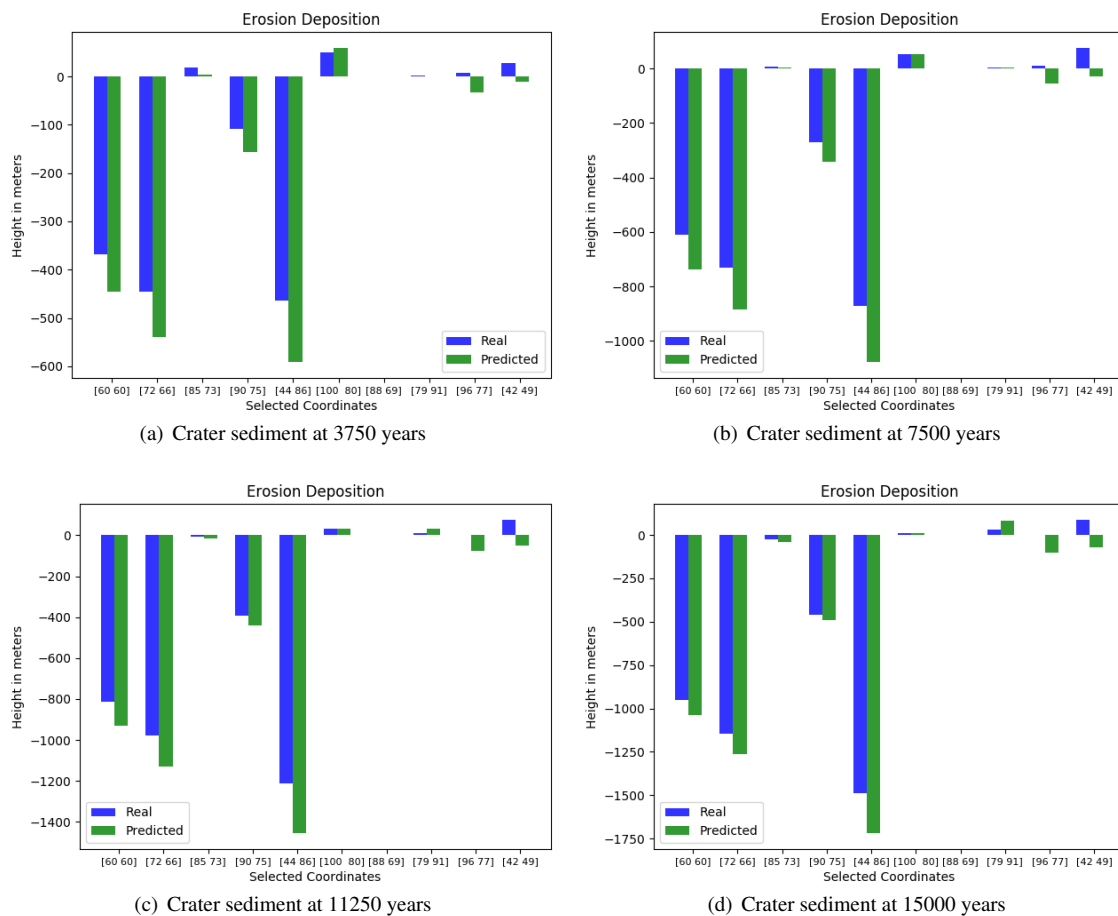


Figure 15: Continental Margin: Sediment erosion and deposition through 15000 years.

- [5] L. R. Scott, S. Zhang, Finite element interpolation of nonsmooth functions satisfying boundary conditions, *Mathematics of Computation* 54 (190) (1990) 483–493.
- [6] V. Godard, J. Lavé, R. Cattin, Numerical modelling of erosion processes in the himalayas of nepal: Effects of spatial variations of rock strength and precipitation, *Geological Society, London, Special Publications* 253 (1) (2006) 341–358.
- [7] J. Rejman, R. Turski, J. Paluszek, Spatial and temporal variations in erodibility of loess soil, *Soil and Tillage Research* 46 (1-2) (1998) 61–68.
- [8] W. K. Hastings, Monte carlo sampling methods using markov chains and their applications, *Biometrika* 57 (1) (1970) 97–109.
- [9] N. Metropolis, A. W. Rosenbluth, M. N. Rosenbluth, A. H. Teller, E. Teller, Equation of state calculations by fast computing machines, *The journal of chemical physics* 21 (6) (1953) 1087–1092.
- [10] A. Jasra, D. A. Stephens, K. Gallagher, C. C. Holmes, Bayesian mixture modelling in geochronology via markov chain monte carlo, *Mathematical Geology* 38 (3) (2006) 269–300.
- [11] D. Raje, R. Krishnan, Bayesian parameter uncertainty modeling in a macroscale hydrologic model and its impact on indian river basin hydrology under climate change, *Water Resources Research* 48 (8).
- [12] M. Thyer, D. Kavetski, G. Evin, G. Kuczera, B. Renard, D. McInerney, Bayesian analysis diagnostics: Diagnosing predictive and parameter uncertainty for hydrological models, in: *EGU General Assembly Conference Abstracts*, Vol. 17, 2015.
- [13] L. Gaál, J. Szolgay, S. Kohnová, K. Hlavčová, A. Viglione, Inclusion of historical information in flood frequency analysis using a bayesian mcmc technique: a case study for the power dam orlík, czech republic, *Contributions to Geophysics and Geodesy* 40 (2) (2010) 121–147.
- [14] K. Charvin, K. Gallagher, G. L. Hampson, R. Labourdette, A bayesian approach to inverse modelling of stratigraphy, part 1: Method, *Basin Research* 21 (1) (2009) 5–25.
- [15] H. Wang, X. Jin, Characterization of groundwater contaminant source using bayesian method, *Stochastic environmental research and risk assessment* 27 (4) (2013) 867–876.
- [16] A. Malinverno, Parsimonious bayesian markov chain monte carlo inversion in a nonlinear geophysical problem, *Geophysical Journal International* 151 (3) (2002) 675–688.
- [17] K. Mosegaard, A. Tarantola, Monte carlo sampling of solutions to inverse problems, *Journal of Geophysical Research: Solid Earth* 100 (B7) (1995) 12431–12447.
- [18] M. Sambridge, K. Mosegaard, Monte carlo methods in geophysical inverse problems, *Reviews of Geophysics* 40 (3).
- [19] M. Sambridge, Geophysical inversion with a neighbourhood algorithm II. appraising the ensemble, *Geophysical Journal International* 138 (3) (1999) 727–746.
- [20] M. K. Sen, P. L. Stoffa, *Global optimization methods in geophysical inversion*, Cambridge University Press, 2013.
- [21] K. Gallagher, K. Charvin, S. Nielsen, M. Sambridge, J. Stephenson, Markov chain monte carlo (mcmc) sampling methods to determine optimal models, model resolution and model choice for earth science problems, *Marine and Petroleum Geology* 26 (4) (2009) 525–535.
- [22] Z. Chair, P. K. Varshney, Distributed bayesian hypothesis testing with distributed data fusion, *IEEE transactions on systems, man, and cybernetics* 18 (5) (1988) 695–699.
- [23] C. Notarnicola, F. Posa, Bayesian fusion of active and passive microwave data for estimating bare soil water content, in: *Geoscience and Remote Sensing Symposium, 2001. IGARSS’01. IEEE 2001 International*, Vol. 3, IEEE, 2001, pp. 1167–1169.

- [24] W. Moon, C. So, Information representation and integration of multiple sets of spatial geoscience data, in: *Geoscience and Remote Sensing Symposium, 1995. IGARSS'95. Quantitative Remote Sensing for Science and Applications*, International, Vol. 3, IEEE, 1995, pp. 2141–2144.
- [25] C. Fonnesbeck, A. Patil, D. Huard, J. Salvatier, Pymc: Bayesian stochastic modelling in python, *Astrophysics Source Code Library*.
- [26] A. J. Drummond, M. A. Suchard, D. Xie, A. Rambaut, Bayesian phylogenetics with beauti and the beast 1.7, *Molecular biology and evolution* 29 (8) (2012) 1969–1973.
- [27] K. X. Whipple, G. E. Tucker, Implications of sediment-flux-dependent river incision models for landscape evolution, *Journal of Geophysical Research: Solid Earth* 107 (B2) (2002) 1–20.
- [28] G. Tucker, G. R. Hancock, Modelling landscape evolution., *Earth Surf. Process Landf.* 35 (1) (2010) 2850.
- [29] T. Salles, G. Duclaux, Combined hillslope diffusion and sediment transport simulation applied to landscape dynamics modelling., *Earth Surf. Process Landf.* 40 (6) (2015) 82339.
- [30] B. Campforts, W. Schwanghart, G. Govers, Accurate simulation of transient landscape evolution by eliminating numerical diffusion: the ttem 1.0 model, *Earth Surface Dynamics* 5 (1) (2017) 47–66.
- [31] J. M. Adams, N. M. Gasparini, D. E. J. Hobbey, G. E. Tucker, E. W. H. Hutton, S. S. Nudurupati, E. Istanbuluoglu, The landlab v1.0 overland-flow component: a python tool for computing shallow-water flow across watersheds, *Geoscientific Model Development* 10 (4) (2017) 1645–1663.
- [32] A. D. Howard, W. E. Dietrich, M. A. Seidl, Modeling fluvial erosion on regional to continental scales, *Journal of Geophysical Research: Solid Earth* 99 (B7) (1994) 13971–13986.
- [33] D. E. J. Hobbey, H. D. Sinclair, S. M. Mudd, P. A. Cowie, Field calibration of sediment flux dependent river incision, *Journal of Geophysical Research: Earth Surface* 116 (F4).
- [34] T. Salles, Badlands: A parallel basin and landscape dynamics model, *SoftwareX* 5 (2016) 195–202.
- [35] J. Braun, M. Sambridge, Modelling landscape evolution on geological time scales: a new method based on irregular spatial discretization, *Basin Research* 9 (1) (1997) 27–52.
- [36] G. Tucker, S. Lancaster, N. Gasparini, R. Bras, *The Channel-Hillslope Integrated Landscape Development Model (CHILD)*, Springer US, Boston, MA, 2001, pp. 349–388.
- [37] J. Braun, S. D. Willett, A very efficient o(n), implicit and parallel method to solve the stream power equation governing fluvial incision and landscape evolution, *Geomorphology* 180–181 (Supplement C) (2013) 170–179.
- [38] J. F. O’Callaghan, D. M. Mark, The extraction of drainage networks from digital elevation data, *Computer Vision, Graphics, and Image Processing* 28 (3) (1984) 323–344.
- [39] A. Chen, J. Darbon, J.-M. Morel, Landscape evolution models: a review of their fundamental equations., *Geomorphology* 219 (2014) 6886.
- [40] D. E. J. Hobbey, J. M. Adams, S. S. Nudurupati, E. W. H. Hutton, N. M. Gasparini, E. Istanbuluoglu, G. E. Tucker, Creative computing with landlab: an open-source toolkit for building, coupling, and exploring two-dimensional numerical models of earth-surface dynamics, *Earth Surface Dynamics* 5 (1) (2017) 21–46.
- [41] H. Jeffreys, An invariant form for the prior probability in estimation problems, *Proceedings of the Royal Society of London. Series A, Mathematical and Physical Sciences* (1946) 453–461.
- [42] D. J. Earl, M. W. Deem, Parallel tempering: Theory, applications, and new perspectives, *Physical Chemistry Chemical Physics* 7 (23) (2005) 3910–3916.
- [43] M. Sambridge, A parallel tempering algorithm for probabilistic sampling and multimodal optimization, *Geophysical Journal International* 196 (1) (2013) 357–374.